ChemComm

Accepted Manuscript

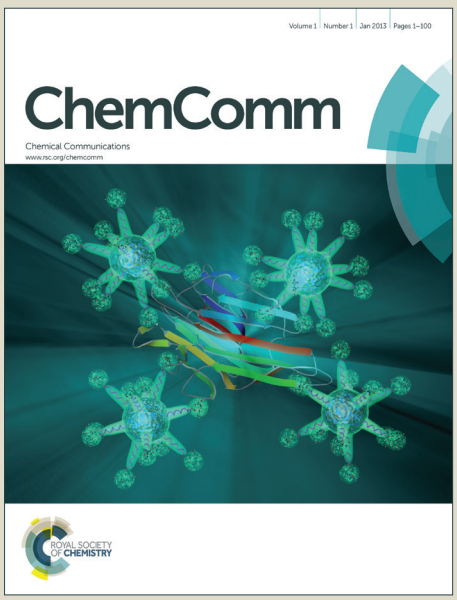

ROYAL SOCIETY OF CHEMISTRY

www.rsc.org/chemcomm

Cite this: DOI: 10.1039/c0xx00000x

www.rsc.org/chemcomm

COMMUNICATION

An Intuitional Hierarchical Assembly of Cluster−Organic Framework with 1.97 nm Thickness from Discrete Co_{14} Cluster†

Fu-Ping Huang,*[a] Peng-Fei Yao,[a] Hai-Ye Li,[a] Qing Yu,[a] He-Dong Bian,*[b] and Hong Liang[a]

Received (in XXX, XXX) Xth XXXXXXXXX 20XX, Accepted Xth XXXXXXXXX 20XX

DOI: 10.1039/b000000x

An intuitional hierarchical assembly, metaphorically referred to as a "blossom and yield fruit" process, from a discrete cluster {[$Co_{14}(CH_3O)_4(dpbt)_6Cl_{12}$]•$14CH_3OH$, (1)} to 2D cluster organic frameworks {[$Co_{14}(CH_3O)_{10}(dpbt)_6Cl_6$]•$12CH_3OH$, (2)}, has been established. The magnetic ordering of 2 were improved obviously compared with 1.

Polynuclear coordination clusters and metal−organic frameworks are two families of functional materials that are fascinating due to their enormous potential in envisioned technological applications in heterogeneous catalysis, host-guest chemistry, nanotechnology and magnetic materials.[1,2] Of particular interest is combining the structural features and functionality of both clusters and MOFs, as this would allow the creation of a special class of cluster−organic frameworks (COFs) with unusual topologies and a strong size dependency, different from those of the corresponding bulk materials and the lower nuclearity clusters.[3] The study of the assembly and reactivity of nanosized clusters has also emerged as an exciting new branch of supramolecular chemistry.[4] While remarkable successes have been made, and "hierarchical assembly" hypotheses have been invoked by Yaghi, Férey, Zaworotko, Zhou, et al, to illuminate the mechanism of the assembly of porous MOFs, starting from polyhedral cluster cores. There exists very little overlap between the two for the insoluble intermediate polynuclear clusters.[5,6]

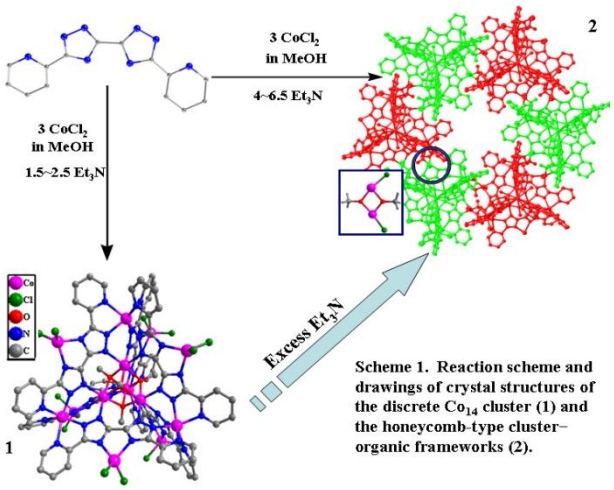

Scheme 1. Reaction scheme and drawings of crystal structures of the discrete Co_{14} cluster (1) and the honeycomb-type cluster−organic frameworks (2).

An interesting observation is the incorporation of small anionic species in many nanosized clusters so-obtained. These include halides, oxide, hydroxide and methoxo, either present in the original reaction mixture or generated in *situ* due to hydrolysis/alcoholysis reactions. These species are good bridginggroups to aggregate metals and a series of impressive giant clusters, consisting of Fe_{64}, Mn_{84}, Co_{32}, Er_{60}, $Ni_{54}Gd_{54}$, and $Gd_{12}Mo_4$, had been isolated.[7-10] Likewise, these species contribute to the exciting cluster growth and studies have established their indispensible role in templating the assembly of the clusters.

We reported here the self-assembly of a discrete [Co_4⊂Co_{10}] cluster with T_d symmetry, [$Co_{14}(CH_3O)_4(dpbt)_6Cl_{12}$]•$14CH_3OH$ (**1**) as blue-green strip crystals, obtained by a solvothermal reaction using a mixture containing a new bis-triazolate ligand 5,5'-di(pyridin-2-yl)-3,3'-bi(1,2,4-triazole) (H_2dpbt), $CoCl_2·6H_2O$ and triethylamine in methanol/ethanol at 130 °C for 72 h. **1** self-assembles from lower concentrated triethylamine (Et_3N) solution, while at high concentrations, a novel cluster-based framework, namely, [$Co_{14}(CH_3O)_{10}(dpbt)_6Cl_6$]•$12CH_3OH$ (**2**) as yellow hexagon crystals, has been isolated. Remarkably, **2** features a novel example of honeycomb-type assembly from the large Cluster-Based Units (CBU), showing a nanosheet with thickness

of *ca*. 1.97 nm. We also show whether changing the concentration of the triethylamine solution can drive structural transformation between **2** and **1** (Scheme 1). Starting from as-prepared sample of **1** and high concentrated triethylamine in methanol, interestingly, the procedure of the conversion from **1** to **2** have been tracked by SEM (Scanning Electron Microscope).

Single-crystal X-ray diffraction studies show that the $[Co_{14}(CH_3O)_4(dpbt)_6Cl_{12}]$ unit in **1** consist of three types of Co centers according to their coordination modes (Fig. S2-3 in the Supporting Information): Four inner Co atoms in distorted N_3O_3 octahedral environments lie at the vertices of the distorted cubic $[Co_4(CH_3O)_4]$ core, held together tightly by four μ_3-CH_3O^- groups, the intracube Co−O distances range from 2.095(5) to 2.156(5) Å, the Co−O−Co angles range from 95.6(2) to 98.7(2)°, and the Co···Co distances are 3.168(1)−3.207(1) Å, respectively. Another four ambient Co atoms in distorted N_6 octahedral environments, are coordinated by six dpbt ligands, to form a classical M_4L_6 cage with T_d symmetry,[11-12] binding the $[Co_4(CH_3O)_4]$ core. The rest of six ambient Co atoms in distorted N_2Cl_2 tetrahedron, are coordinated by six dpbt ligands, and twelve Cl^- anions. The cubic Co_4 core, are bridged to exterior ten Co atoms, through six dpbt ligands, resulting in the discrete Co_{14} cluster in which a cubic Co_4 core is encapsulated by a Co_{10} adamantane periphery. In the reactive system of **1**, CH_3O^- species aggregate metal centers to form $[Co_4(CH_3O)_4]$ core. Remarkably, by employing higher concentrated Et_3N solution, the adjacent Co_{14} clusters are mutually interdigitated and two of the metal vertices are further linked by two CH_3O^- species to yield a honeycomb-type nanosheet of **2**, with 1.97 nm thickness. Presumably the pH environment is the driving force behind the formation of the cluster−organic framework. Switching by employing the same starting materials but Et_3N range from 1.5~2.5 and 4~6.5 equiv per dpbt, resulted in pure **1** and **2**, respectively. It is well known that there exists abundent CH_3O^- anionic species, when excess Et_3N was added into methanol, due to the alcoholysis reactions. In the current case, the CH_3O^- species forces the Co_{14} clusters to aggregate and leads to the formation of two $[Co_2(CH_3O)_2]$ units between a pair of adjacent Co_{14} clusters, thereby extending the structure to a novel cluster−organic framework (Fig. S4-5). Keeping these considerations in mind, we set out to investigate whether changing the concentration of the Et_3N solution can drive the structural transformation between **2** and **1**.

We immersed a few blue-green samples (*ca*. 20 mg of single crystals) of **1** in a sufficient amount of a methanol solution of Et_3N in a small sealed vial at room temperature, and we observed that the crystals of **1** get noticeably lighter. Although the strip crystals retained their original external forms, there action proceeded and **2** was eventually produced (Fig. 1). SEM reveals that there are hexagon patterns gradually generated on the surface of the strip crystals of **1**. The growth of hexagon crystals on **1** allow to form the crystal(hexagon)-on-crystal(strip) phase in this case (Fig. 1d-e). As time goes on, some attached shell hexagon crystals separated themselves from strip crystal of **1**. The crystals were picked out and washed with MeOH solvent. To probe the structural information of the grown crystals on **1**, we cut the outer parts of the composite crystal(hexagon)-on-crystal(strip) system carefullly and performed X-ray crystallography. The Powder X-ray diffraction (PXRD) studies of the outer part, and the subsequent X-ray single-crystal diffraction of the generated hexagon crystal unveiling that the shell crystal is **2** (Fig. S8). Note that the solvothermal reaction with **1** in this reaction condition can also produced **2**, further confirmed the conversion of **1** to **2**.

2 crystallizes in trigonal system, space group *P*-3, showing a novel nanocluster-based layer structure, in which the metal vertices of the adjacent clusters are mutually interdigitated from three different orientation, to form a honeycomb-type nanosheet with thickness of *ca*. 19.7 Å, leaving hexagon windows. The mutually interdigitation of adjacent Co_{14} clusters make **2** more stable than **1**. When suspended in CH_2Cl_2/MeOH (with a volume ratio of 1:2), **2** dissolved slowly to give a teal solution. The electrospray mass spectrometric experiment of **2** was taken to explore their solution stability. The ESI-MS and HPLC-MS of **2** exhibits a series of double charged ion peaks in the range of *m/z* = 765-776 and trivalent peaks in the range of *m/z* = 1147-1165. Through assigning the fragment ions observed in the MS, and by analysing the structural features of the Co_{14} cluster, we were able to propose that the dissociation of the nanosheet into discrete species of $[Co_8((OH)_x(CH_3O)_y(dpbt)_6+3H]^{3+}$ and $[Co_8((OH)_x(CH_3O)_y(dpbt)_6+2H]^{2+}$ (x = 0-2, y = 2-4) (Fig. S9-10), which presumably having a aforementioned Co_4L_6 cage binding the $[Co_4(CH_3O)_4]$ core. And OH^-/CH_3O^- substitution reaction maybe happened in the $[Co_4(CH_3O)_4]$ unit, due to solvation effect.[13-14] The isotope distributions closely match the simulated patterns, confirming the Co_8 composition, which derived from de-$(CoCl_2)_6$ of **1.**

On the basis of these experiment results, the conversion mechanism maybe proposed: Cl^- can diffuse and be exposed on the surface of **1**, where they are slowly replaced by CH_3O^- ions from the alcoholysis reactions. The exchange takes place on the entire surface. The crystals of **2** begin to seed on the surface. Further diffusion of CH_3O^- ions allows the formation of the flower-typed hexagon patterns and the crystal(hexagon)-on-crystal(strip) hybridized system. The newly formed crystals are then aggregated onto the **2** crystals rather than onto a new surface of **1** because the already grown crystals can serve as seeds. In the termination step, the seeds of **1** are completely aggregated and the single crystals attached to **1** are librated to give the final **2** crystals. The overall process can be metaphorically referred to as a "blossom and yield fruit" course. The type of stimuli-responsive synthetic strategy in response to environmental changes, maybe future applied in mimicking the aggregation of giant nanoclusters with single molecule magnet (SMM) behavior and membrane formation.[15-16] It also provides us a new synthetic strategy to achieve higher dimensional hierarchical assembled arrays, showing interesting magnetic property, in response to environmental changes such as solvent, temperature, and pH. [17-18]

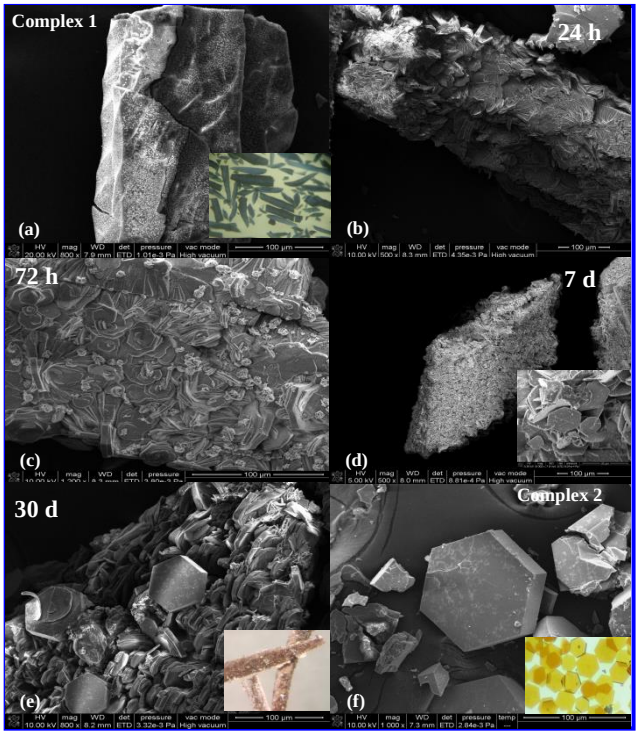

Fig. 1. Scanning electron microscopy(SEM) images (100 μm) of complex **1** (a), **2** (f) and **2/1** phase (b-e). Insets are the Photographs of **1** (a), **2** (f), **2/1** (e), and the magnified SEM image (20 μm) showing the growth of the hexagon crystals (d).

As anticipated, the temperature dependent magnetic susceptibilities of **1-2** were measured with an applied field of 1000 Oe for the fresh samples were displayed in Fig. 2. The $\chi_M T$ values decrease gradually from the room-temperature value of 38.08 and 40.94 $cm^3 \cdot K \cdot mol^{-1}$ to 4.74 and 3.24 $cm^3 \cdot K \cdot mol^{-1}$ at 2 K for **1-2**, respectively. The reciprocal molar susceptibilities in 20–300 K follow the Curie–Weiss Law of $1/\chi_M = (T-\theta)/C$ with Curie constants C = 42.86 and 48.59 $cm^3 \cdot K \cdot mol^{-1}$ and Weiss Constants θ = -34.06 K and -53.64 K for **1-2**, respectively. The negative θ values suggest an antiferro-magnetic interactions between the metal centers and/or the spin–orbit coupling effect of Co(II). The larger $|\theta|$ of **2** than that of **1** may be mainly attributed to the presence of the double μ_2-CH_3O^- bridges, which significantly enhance the inter-clusters antiferromagnetic interaction of **2.**

To compare the magnetic behavior roughly yet directly with those in **1**, FC magnetizations of **1-2** were measured under different applied fields. The magnetic behavior of **2** is more markedly field-dependent, suggests that the local spins adopt a spin-canting configuration. Further characterization of the weak ferromagnetism in **2** shows a hysteresis loop observed at 2 K with a coercive field of 101 Oe per cluster and an obvious *ac* susceptibility signal from 4 to 9 K. This behavior confirms the presence of the long-range order in **2**. Although there is observable field-dependent behavior, **1** keep silent in hysteresis loop and *ac* susceptibility measurent in the corresponding temperature. Thus in **2**, the coexistence of spin canting and long-range magnetic ordering observed at 4-9 K, may be mainly attributed to the presence of the inter-clusters double μ_2-CH_3O^- bridges, which have no inversion center but aggregate adjacent Co_{14} clusters to higher dimensional hierarchical assembly.[19]

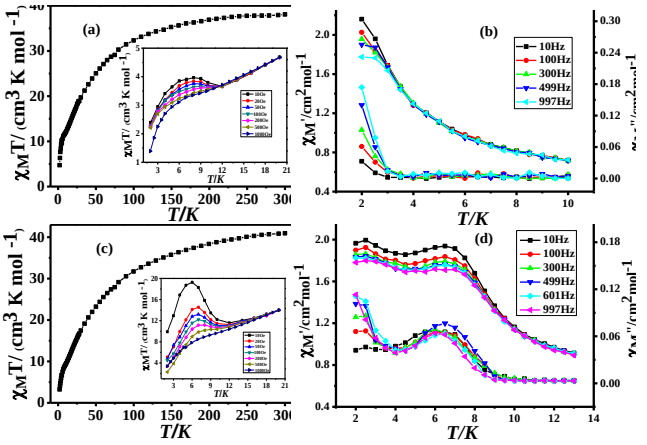

Fig. 2. Temperature dependence of magnetic susceptibility of **1** (a) and **2** (c). Inset: FC magnetization of them in different field. And the in-phase and out-of-phase ac magnetic susceptibilities for **1** (b) and **2** (d).

In summary, an intuitional hierarchical assembly from Co_{14} clusters to 2-D COFs in response to environmental change, has been established. To our knowledge, such "blossom and yield fruit" process in the SCSC (single crystal to single crystal) hierarchical assembly is seldom. The stability and magnetic ordering of **2** were greatly improved compared with those of **1**. More interestingly, the type of stimuli-responsive strategy provides a general implications in the control of assembly of giant nanoclusters with SMM behavior and membrane formation through size augmentation. When soaked into water (Fig. S11), **2** allows exfoliation of itself from the hexagon yellow crystals. It may make **2** an attrative candidate to generate a 2D-polymer, further confirming the nanosheets of **2** are stable in wet air. The preparation of the single nano-layer and detailed studies of their magnetic properties are currently under way.

This work is financially sponsored by the National Nature Science Foundation of China (Nos. 21101035, 21461003 and 21361003), and the Guangxi Natural Science Foundation (2012GXNSFBA053017 and 2014GXNSFBA118056).

Notes and references

a Key Laboratory for the Chemistry and Molecular Engineering of Medicinal Resources (Ministry of Education of China), School of Chemistry and Pharmacy, Guangxi Normal University, Guilin 541004, P. R. China. Fax: +86-773-2120958; E-mail: huangfp2010@163.com

b School of Chemistry and Chemical Engineering, Guangxi University for Nationalities, Nanning, 530008, P. R. China. E-mail: gxunchem@163.com

† Electronic supplementary information (ESI) available: crystallographic data (CIF), Experimental details, Structural Details, Measurement Details and magnetic data. CCDC 1028478 for **1** and 1028479 for **2**. For ESI and

crystallographic data in CIF or other electronic FormatSee DOI: 10.1039/b000000x/

1 (a) H.-C. Zhou, J. R. Long and O. M. Yaghi, *Chem. Rev.* 2012, **112**, 673–674; (b) Q.-L. Zhu and Q. Xu, *Chem. Soc. Rev.* 2014, **43**, 5468–5512.

2 (a) L. Bogani and W. Wernsdorfer, *Nat. Mater.*, 2008, **7**, 179–184; (b) Q.-F. Sun, S. Sato and M. Fujita *Angew. Chem. Int. Ed.* 2014, 53, 13510–13513; (c) D. Fujita, H. Yokoyama, Y. Ueda, S. Sato and M. Fujita *Angew. Chem. Int. Ed.* 2015, **54**,155–158.

3 G. Karotsis, S. Kennedy, S. J. Teat, C. M. Beavers, D. A. Fowler, J. J. Morales, M. Evangelisti, S. J. Dalgarno and E. K. Brechin, *J. Am. Chem. Soc*., 2010, **132**, 12983–12990.

4 (a) J.-R. Li, D. J. Timmons and H.-C. Zhou, *J. Am. Chem. Soc.* 2009, **131**, 6368–6369; (b) J.-R. Li, J. Sculley and H.-C. Zhou, *Chem. Rev.* 2012, **112**, 869–932.

5 (a) H. Chun, *J. Am. Chem. Soc.* 2008, **130**, 800–801; (b) Z.-Q. Xu, Q. Wang, H. J. Li, W. Meng, Y. Han, H. W. Hou and Y. T. Fan *Chem. Commun.*, 2012, **48**, 5736–5738; (c) M. Li, D. Li, M. O'Keeffe and O. M. Yaghi, *Chem. Rev.* 2014, **114**, 1343–1370.

6 (a) Z.-J. Zhang, L. Wojtas, M. Eddaoudi and M. J. Zaworotko, *J. Am. Chem. Soc.* 2013, **135**, 5982–5985; (b) D.-W. Feng, K.-C. Wang, J. Su, T.-F. Liu, J. Park, Z.-W. Wei, M. Bosch, A. Yakovenko, X.-D. Zou and H.-C. Zhou *Angew. Chem. Int. Ed.* 2015, **54**, 149–154; (c) J. Park, D.-W. Feng, S. Yuan and H.-C. Zhou *Angew. Chem. Int. Ed.* 2015, **54**, 430–435.

7 (a) T. Liu, Y. J. Zhang, Z. M. Wang and S. Gao, *J. Am. Chem. Soc.* 2008, **130**, 10500–10501; (b) A. J. Tasiopoulos, A. Vinslava, W. Wernsdorfer, K. A. Abboud and G. Christou, *Angew. Chem., Int. Ed.* 2004, **43**, 2117–2121.

8 Y.-F. Bi, X.-T. Wang, W.-P. Liao, X.-F. Wang, X.-W. Wang, H.-J. Zhang and S. Gao *J. Am. Chem. Soc.*, 2009, **131**, 11650–11651.

9 Y.-Q. Hu, M.-H. Zeng, K. Zhang, S. Hu, F.-F. Zhou and M. Kurmoo, *J. Am. Chem. Soc.* 2013, **135**, 7901–7908.

10 (a) X.-J. Kong, Y. Wu, L.-S. Long, L.-S. Zheng and Z. Zheng, *J. Am. Chem. Soc.* 2009, **131**, 6918–6919; (b) Y. Zheng, Q. C. Zhang, L. S. Long, R. B. Huang, A. Müller, J. Schnack, L. S. Zheng and Z. P. Zheng, *Chem. Commun.*, 2013, **49**, 36–38.

11 R. W. Saalfrank, H. Maid and A. Scheurer, *Angew. Chem., Int. Ed.* 2008, **47**, 8794–8824.

12 (a) R. Custelcean, P. V. Bonnesen, N. C. Duncan, X. H. Zhang, L. A. Watson, G. V. Berkel, W. B. Parson and B. P. Hay, *J. Am. Chem. Soc.* 2012, **134**, 8525–8534; (b) S. Yi, V. Brega, B. Captaina and A. E. Kaifer, *Chem. Commun.*, 2012, **48**, 10295–10297.

13 (a) G. N. Newton, G. J. T. Cooper, P. Kögerler, D. L. Long and L. Cronin, *J. Am. Chem. Soc.* 2008, **130**, 790–791; (b) D. O. Sells, E. J. L. McInnes and L. Cronin, *J. Am. Chem. Soc.* 2012, **134**, 6980–6983.

14 F. Xu, R. A. Scullion, J. Yan, H. N. Miras, C. Busche, A. Scandurra, B. Pignataro, D.-L. Long and L. Cronin, *J. Am. Chem. Soc*. 2011, **133**, 4684–4686.

15 (a) G. Bozoklu, C. Gateau, D. Imbert, J. Pecaut, K. Robeyns, Y. Filinchuk, F. Memon, G. Muller and M. Mazzanti *J. Am. Chem. Soc.* 2012, **134**, 8372–8375; (b) X.-P. Zhou, Y. Wu and D. Li, *J. Am. Chem. Soc.* 2013, **135**, 16062–16065.

16 (a) T.-F. Liu, Y.-P. Chen, A. A. Yakovenko and H.-C. Zhou, *J. Am. Chem. Soc.* 2012, **134**, 17358–17361; (b) K. Otsubo, T. Haraguchi, O. Sakata, A. Fujiwara and H. Kitagawa, *J. Am. Chem. Soc.* 2012, **134**, 9605–9608.

17 (a) X. N. Cheng, W. X. Zhang and X. M. Chen, *J. Am. Chem. Soc.* **2007**, 129, 15738-15739; (b) W. R. Lee, D. W. Ryu, W. J. Phang, J. H. Park and C. S. Hong *Chem. Commun.*, 2012, 48, 10847–10849; (c) S. Yi, V. Brega, B. Captain and A. E. Kaifer *Chem. Commun.*, 2012, **48**, 10295–10297; (d) M. Wriedt, A. A. Yakovenko, G. J. Halder, A. V. Prosvirin, K. R. Dunbar and H.-C. Zhou, *J. Am. Chem. Soc.* 2013, **135**, 4040–4050.

18 (a) Y.-F. Bi, W.-P. Liao, G.-C. Xu, R.-P. Deng, M.-Y. Wang, Z.-J. Wu, S. Gao and H.-J. Zhang, *Inorg. Chem.* 2010, **49**, 7735–7740; (b) G. N. Newton, K. Mitsumoto, R. J. Wei, F. Iijima, T. Shiga, H. Nishikawa and H. Oshio, *Angew. Chem. Int. Ed.* 2014, **53**, 1–5.

19 (a) M. Kurmoo, *Chem. Soc. Rev.*, 2009, **38**, 1353-1379; (b) X.-Y. Wang, Z.-M. Wang and S. Gao *Inorg. Chem.*, 2008, **47**, 5720–5726.